Chapter 9

Numerical Study of Support Interferences on the SOAR Separation Wind Tunnel Test

Alberto Ghiraldo, Sebastien Paris and Ernesto Benini

Additional information is available at the end of the chapter

http://dx.doi.org/10.5772/62241

Abstract

A process of support design for wind tunnel models and the evaluation of interferences effect are described in this chapter. The work was performed at the Von Karman Institute for Fluid Dynamics (VKI; Sint-Genesius-Rode, Belgium), and it was commissioned by the S3-Swiss Space System company. The work concerns the separation wind tunnel test of the Suborbital Aircraft Reusable (SOAR) vehicle from an Airbus commercial plane carrier. The supports are designed for future separation wind tunnel test of the SOAR version V10 in the VKI-S1 wind tunnel. They are designed in scale 1:180 for the test of the SOAR in the presence of the Airbus and in scale 1:80 for the SOAR alone test. Two different shapes of support (circular and elliptic) are tested in each case. First there are the supports designed, then the results of the finite element method (FEM) static structural analysis and vibrational analysis, and finally the result of the computational fluid dynamics (CFD) campaign. The flow and the force interferences caused by the support are investigated by comparing simulations with and without support. The behavior of the two shapes and of the dimensional variations are investigated at an angle of attack between 0° and 15° and at Mach 0.7.

Keywords: separation wind tunnel test, SOAR, support design, support interferences, VKI

1. Introduction

Theoretical aerodynamic study, computational fluid dynamics (CFD) analysis, and wind tunnel tests are the three pillars of every aerodynamic design process. In this paper, the emphasis is on how CFD and theoretical study can be complementary and how to prepare the wind tunnel test.

The present project, commissioned by the S3-Swiss Space System, deals with the development and qualification of three stages to orbit a composite vehicle. The first and second stages, the Airbus and the Suborbital Aircraft Reusable (SOAR) vehicles, respectively, are reusable, whereas the third stage is an expandable booster. All details of the SOAR mission are in Ref. [1].see **Figure 1** This project requested the design of new supports for the separation wind tunnel test in the VKI facility and the study of the respective interferences.

The S3 SOAR separation from the Airbus A300 is a critical issue during the mission. The aerodynamic coefficients are affected by the proximity of the vehicles. To correctly design the separation, the aerodynamic database must be known with sufficient accuracy. For this reason, an important campaign of wind tunnel testing is necessary.

An earlier wind tunnel campaign had already been performed with the construction of an initial aerodynamic database [2]. To carry out further wind tunnel experiments, an improvement in the knowledge of support design is required. In fact, to design supports for the SOAR, in this configuration, is particularly complicated due to the presence of the Airbus below and behind the vehicle (the A300 empennage also impedes the use of a support from the base). Effectively, the first sting designed produced considerable interferences on the model. Therefore, the purpose of this work is to design supports for the SOAR vehicle in the following two configurations: scale 1:180 for the wind tunnel test of the SOAR in the presence of the Airbus and scale 1:80 for the wind tunnel test of the SOAR alone.

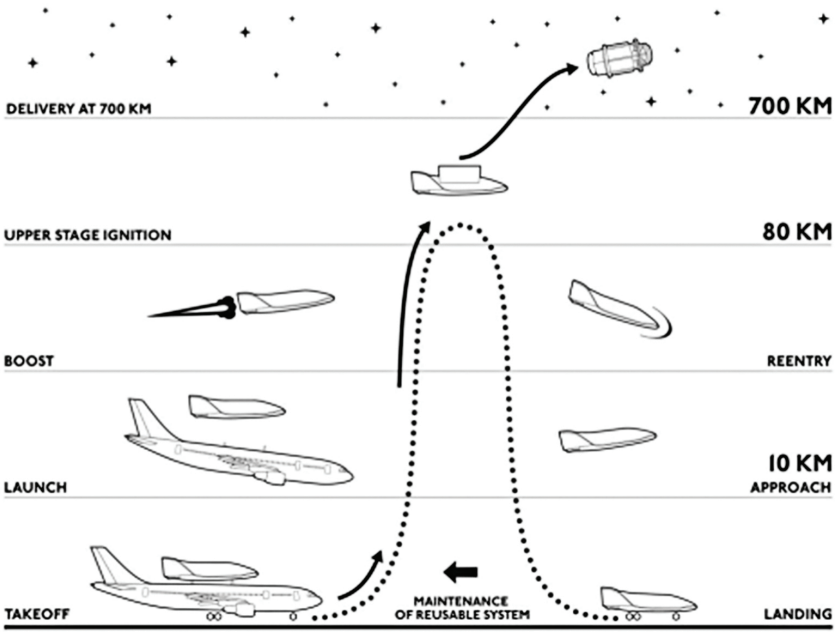

Figure 1. Illustration of the main steps of the mission.

http://dx.doi.org/10.5772/62241

2. Support design

The support in wind tunnel tests is necessary to hold up the model in the test section, but it is also an artificial device that, especially from an aerodynamic point of view, does not exist. From this definition, the following design constraints are immediately derived: to minimize the aerodynamic interferences with the flow ensuring adequate mechanical properties to sustain the model. It is also necessary to consider the wind tunnel test conditions (M=0.7, α_{max}=15°), the model shapes, and the use of steel as material for the supports. Furthermore, the support has to allow the internal passage of cables that interface the 6 degrees of freedom internal balance with the measurement device. Finally, the test section dimensions of the VKI-S1 wind tunnel (0.4×0.36 m) and the need to adopt a new configuration with respect to the previous one are considered. This is because the use of a dorsal strut (see **Figure 2**) did not provide satisfactory results regarding the interferences with the models. Some additional constraints are present in scale 1:180 composite testing: to test the separation with the presence of the Airbus empennage and to consider the nominal relative position of the two vehicles. This is necessary to permit a relative motion of the SOAR over the Airbus.

Once requirements about flow measurement and passage of cables are acquired, the two parameters to be optimized are to minimize the aerodynamic interferences and to give adequate mechanical properties.

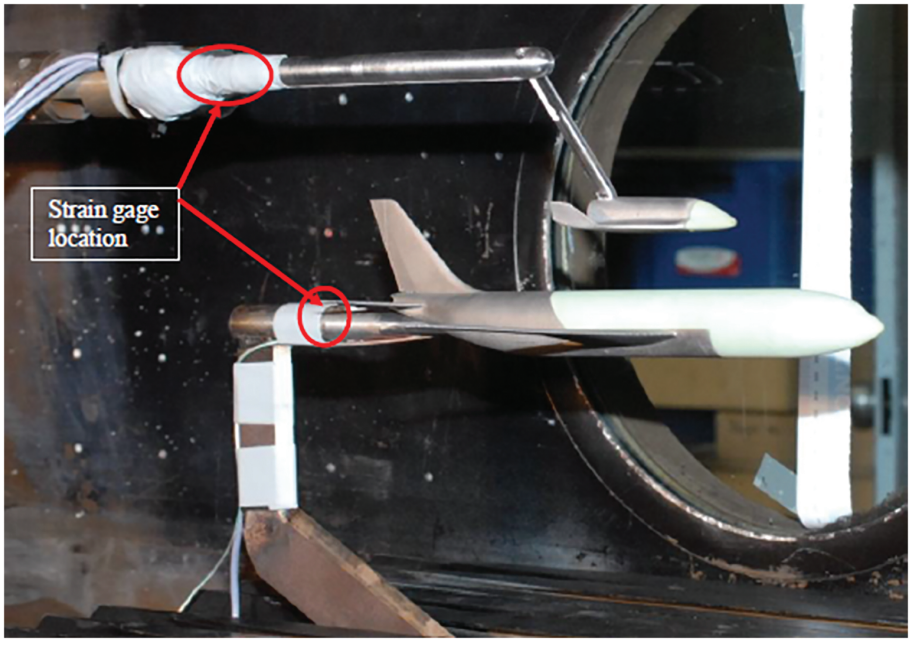

Figure 2. Picture of the old support used in the first separation wind tunnel test.

In fact, to minimize interferences, the sting has to be as long as possible and with the diameter as small as possible. These requirements are not in agreement with the structural properties for which stings should be short and have a large diameter. An important parameter in this dissertation is the "critical sting length" that is "the shortest sting length, which does not change the level of an aerodynamic measurement obtained with longer stings" [3]. The critical sting length is influenced by the Mach number, Reynolds number, boundary layer at the base of the model, sting, and model base diameter. The Reynolds number plays an especially important role. In fact, if the flow is laminar at the base of the model, L_c is as much as 12 to 15 times the base model diameter (D); on the contrary, with turbulent flow, L_c is reduced to 3–5·D.

It is necessary to pay attention that the diameter does not have to modify the typology of the boundary layer at the model base. The minimum diameter allowable, from load considerations, is approximately 0.25 times the model base diameter [4]. For the maximum value, it is necessary to consider that, in the transonic flow, minimum interferences exist with a sting diameter up to 0.4 times the base [5].

In this flow field, the common choice is to use a "straight sting," which is the best solution to reduce the interferences. This is a tube that enters the model at the base. With this choice, all the supporting structure is downstream of the model and it is used with an internal balance system [6].

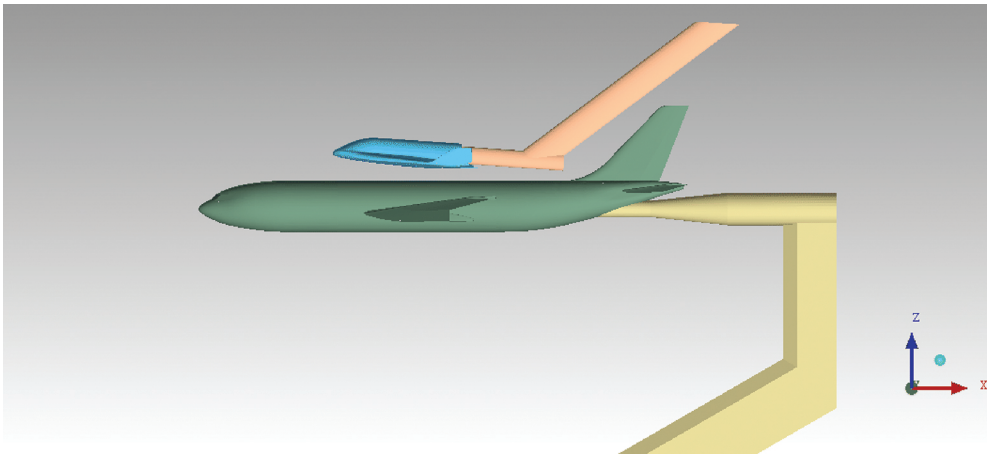

Figure 3. The SOAR (light blue) with the new support (orange) over the Airbus (dark green) in the nominal position; scale 1:180.

The use of a straight sting is possible only for the scale 1:80 model, see **Figure 3** whereas the presence of the Airbus, with its empennage, in the composite configuration (scale 1:180) prevents its usage. see **Figure 4** The only remaining possibility, in this case, is to use a straight sting that enters in the SOAR base (rear surface) but at the other extremity is connected with an inclined bar before the Airbus empennage. The presence of the cables inside the support

http://dx.doi.org/10.5772/62241

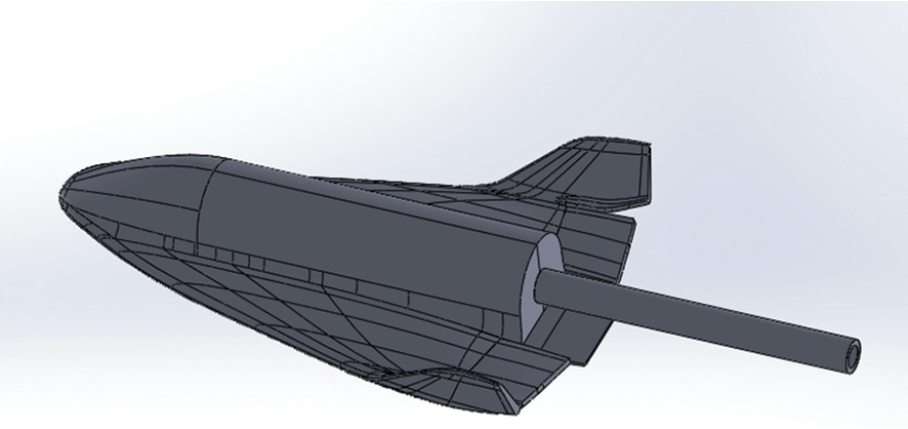

Figure 4. The SOAR with the new circular sting; scale 1:80.

needs a cavity that decreases the stiffness, with the necessity to pay particular attention to the thickness of the walls. From the definition of the critical Reynolds number, it is possible to see that, for the scale 1:80, the flow at the base is definitely turbulent, whereas, in scale 1:180, the transition is around the base. In any case to design a sting 12 to 15 times the length of *D* is not possible due to the constraint of the Airbus empennage, and the longest one possible was designed.

Also, for the diameter, in scale 1:180, it was not possible to respect the rules explained for the presence of the cable inside, and again the smallest one possible was chosen.

The inclined part of the support is clearly a critical point for the interferences and it dramatically breaks the flow in the proximity of the rear portion of the SOAR. For this reason, it made it as less as possible inclined (*B* angle small) with respect to the constraint of the empennage angle (otherwise the support would approach the tail of the Airbus too closely). Another solution, adopted to try to have small interferences, is to use an airfoil shape as section of the inclined bar. In fact, in the transonic flow, a thin airfoil allows for a dramatic reduction of the drag [7]. The aim of this is to choose the thinnest airfoil possible, which is compatible with the structural constraints and the presence of cables inside. The choice was a NACA 0016 cut in the rear part.

Two different shapes of sting sections are evaluated in this work: circular and elliptic. The circular one is the most common and there are many references in the literature [3,4,6]. On the contrary, an elliptic sting should reduce the interferences and the drag especially at a high angle of attack [8]. These configurations will be evaluated at every step of the design process, first from a structural point of view and then with a flow analysis using a CFD software. Because there is a lack of literature on the use of the elliptic sting, its use and the possible advantages of this choice are investigated in depth. All support dimensions are in Ref. [9].

3. Structural analysis

To evaluate the reaction of different supports at the external loads present in the wind tunnel, a static structural analysis and a vibrational analysis were performed [finite element method (FEM)].

For the static structural analysis, the contribution of drag, lift, pitching moment, and lateral forces was taken into account. From this study, although it results that the external loads do not involve compromising stresses, strains, and displacements, it is necessary to highlight two critical points. The first one is that the bending angle due to the displacement at the free extremity, where the model will be connected, is often relevant, especially in scale 1:80. In all cases (circular and elliptic sections, scales 1:80 and 1:180), it is necessary to take into account this bending angle, with an accurate measurement, to have the exact inclination of the model. The second interesting consideration concerns the larger stress (Von Mises) concentrations present with the elliptic sting. The worse behavior of the elliptic shape is because it has a worse filling. In fact, to fit the same cables, it is necessary to reduce the thickness of the wall; otherwise the length of the major semi-axis would have been too large. Both problems are manageable, but they require attention.

With the frequency analysis, it was verified that the external excitation during the experiments is far enough from the resonance frequency of the supports. The main vibrational external disturbance for the stings is the frequency of the vortex shedding of the SOAR model. Thus, the utilization of an elliptic section is possible, but it needs more vigilance regarding the designing of the wall thickness with an increase of the overall dimensions.

4. CFD analysis

The CFD simulations represent the most important contributions in this project. In fact, the flow field and the force interferences due to the support were studied by comparing simulations with and without support. To study the alterations of the flow during the wind tunnel test due to the presence of the artificial strut is fundamental for two reasons: to help design it as discretely as possible and to understand the appropriate correction to the wind tunnel results. In particular, the impact of the different shapes of stings (circular and elliptic), the dimensions, the presence of an inclined part (with different inclinations), and the effect of an angle of attack were studied. Every shape of support (circular or elliptic) was tested, with the nominal dimensions, connected to the vehicle, at angles of attack of 0°, 5°, 10°, and 15°. After this, the variation of the dimensions was evaluated at 0°, with the sting longer or shorter by 10%. In addition, simulations with the diameter bigger than 10% were performed but not with a smaller one, which is not possible if the cables are to be bunched inside the sting. A change in the dimensions (10% length and diameter increase) is applied also with the presence of an angle of attack to understand how these two different aspects can interact. The effect of the inclined part (scale 1:180) was studied by simulations with the nominal inclination of the

http://dx.doi.org/10.5772/62241

vertical part compared to the straight sting (40.8°) and adding 5°, 10°, and 15° of inclination, respectively.

4.1. Pre-processing operations

All meshing operations were done using Ansys ICEM CFD version 15.0, whereas the selected CFD tool was Metacomp CFD++ version 14.1. The computations were performed on the ClusterVision cluster of the VKI.

The unstructured triangular surface mesh was realized using the autoblock method. Elongation surfaces were inserted near the SOAR trailing edge to delay the boundary layer to tetra mesh transition away from the body. This ensured compromising pressure jumps, and it might appear far from the trailing edge due to element transitions. From this surface, a tetra mesh see **Figure 5** mixed with a Delauny method volume mesh was built between the model and the fluid domain walls. After this, an exponential "prism growing" extrusion method was applied, which is a kind of a level-set technique to grow constant thickness layers around the body (with increasing thickness layer by layer). This prism layer forms the boundary layer thickness and it consists of 25 levels with an expansion ratio of 1.2 and first cell height of 0.5 mm. During growth, a directional smoothing and a smoothing of the first layer were applied. Some pyramid elements were generated to connect the prism column end sides to the tetra mesh. Because the target Mach number was lowered to 0.7, it went below the critical Mach number; therefore, shock refinement became unnecessary for this study. However, very small pockets of supersonic flows were observed with Mach number less than 1.1. The total number of mesh elements is just over 1.4 million.

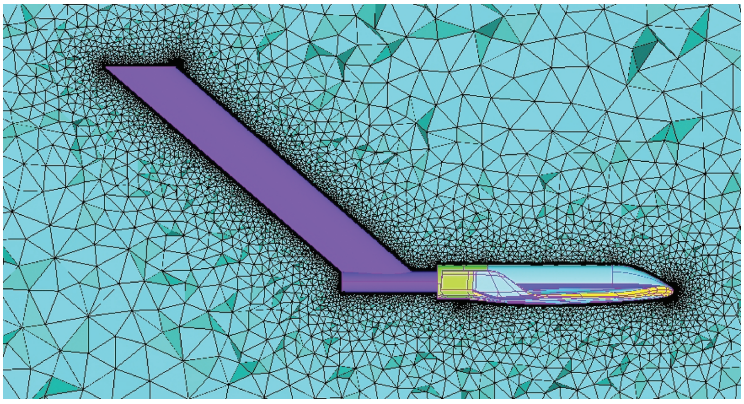

Figure 5. Solid and wire view of the completed volume mesh symmetry plane.

In CFD++, the RANS simulations were performed with the k-ω SST model. All simulations were at M=0.7 and with the wind tunnel set-up [9]. The body-support intersection is quite large; therefore, its effect could not be neglected. The open part would behave as a zero pressure region if not corrected. Hence, the following correction was applied: around the holes of the

SOAR, where the support attaches to the body, the average pressures were computed. Based on these pressures and on the area of the hole, it is possible to introduce a compensating axial force see **Figure 6**.

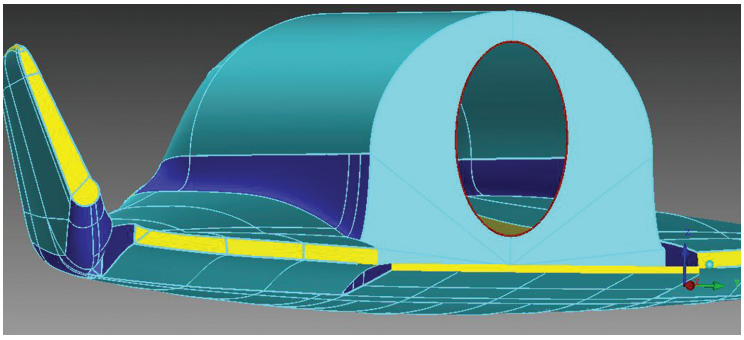

Figure 6. View of the SOAR with the hole for the support. The support correction is based on the average pressure on the red line.

4.2. Result of the CFD analysis

The results were evaluated by looking at the flow topology and at the aerodynamic forces and coefficients database. A summary of the result is presented in the following paragraphs, the complete analysis is in Ref. [9].

4.2.1. Scale 1:180

The origin of the interferences on the model is twofold. The presence of the support blocks the flow in the wake, decreases the recirculation, and increases the pressure that pushes the body forward, reducing the drag. Furthermore, the blockage of the flow in the narrow space between the flap surfaces and the sting generates an extra pressure on the flaps. Because this downward push on the flaps is far from the vehicle's center of gravity (CoG), it causes a considerable increase on the pitching moment. Second, the inclined bar of the support breaks the flow towards the SOAR, especially on the upper surfaces. This generates over pressures on the body and, again, on the flaps responsible for the lift decrease and a contribution in the growing of the moment.

Moreover, the lower surface of the vehicle reveals a higher pressure, but the values are lower than those on the upper part and arranged more homogenously. Then, the higher pressure on the bottom rather contrasts the decrease of the lift but less the increase of the pitching moment.

Now focusing on the effect of different sting shapes, the elliptic one with its more streamlined cross-section causes fewer interferences allowing a better ease of the flow moving around. In particular, this phenomenon is present below the circular sting that, with its larger section, stops the flow more. Furthermore, the circular sting induces a larger vortex on its top.

http://dx.doi.org/10.5772/62241

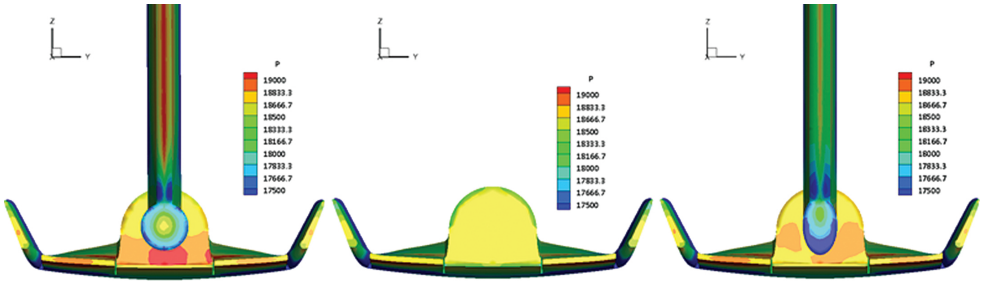

Figure 7. Rear surface view of the SOAR with circular sting on the left, alone in the middle, and with elliptic one on the right; scale 1:180, α=0°.

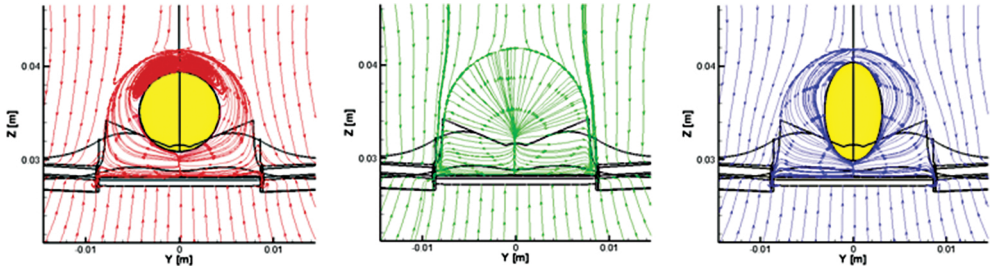

Figure 8. Plot of the y and z velocity components; the SOAR with circular sting on the left, alone in the middle, and with elliptic one on the right; scale 1:180, α=180°.

The impact of these flow alterations on the SOAR coefficients is minimal concerning the drag and the lift, with small angles of attack, for both shapes and it increases at 15°. Raising α the interferences usually growth, less using the elliptic section, that is now clearly advantageous, especially on the lift. On the contrary, for the moment coefficient, the interferences are more important also at small angles presenting a linear increase with the angle of the flow. Even in this case, the usage of an elliptic sting produces less interference. In **Table 1**, there is the average correction on the SOAR alone coefficient, for values of α between 0° and 15°, in scale 1:180. The correction is calculated as the value of the coefficient when the SOAR was alone, minus the value of the same coefficient, only for the SOAR, in a simulation where the support was also present.

Simulations	$\Delta C_{L\,av}$	$\Delta C_{D\,av}$	$\Delta C_{M\,av}$
SOAR with circular sting	0.00590	0.00928	−0.03831
SOAR with elliptic sting	0.00451	0.00703	−0.03425

Table 1. Average correction, respect of the angle of attack, on the coefficients when the support is present compared to the SOAR alone; scale 1:180

To understand the impact of different dimensions on the sting performance, 10% alterations were chosen on the length (longer and shorter) and on the diameter (only larger) see **Figure 9**. It is clear that a shorter sting presents higher interferences with respect to a longer one. In fact, the shorter one induces a higher pressure on the model rear surface and an overpressure on the upper surface and on the flaps. This last fact is due to the greater proximity of the vertical part of the support that breaks the flow over the vehicle.

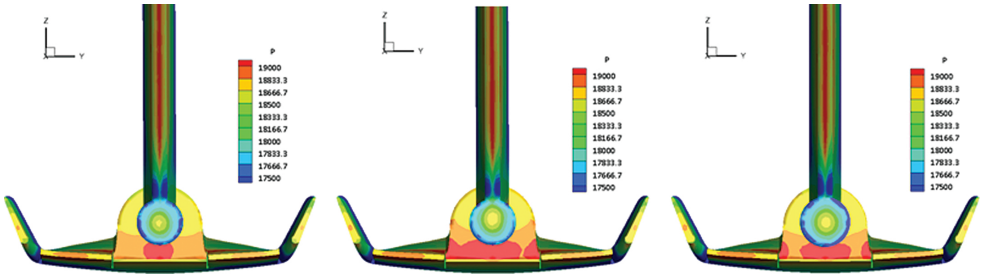

Figure 9. Rear surface view of the SOAR with the sting 10% longer on the left, 10% shorter on the middle, and with the bigger diameter on the right; scale 1:180, α=0°.

It is interesting that a 10% length reduction produces larger changes than a 10% increase. In fact, regarding lift and drag, the effect on the coefficients is smaller when the sting is longer (4–10% interferences see **Table 11** reduction) but more important when it is shorter (30–40% interferences increases) with respect to the nominal dimensions. This does not happen for the circular sting drag coefficient where it is the opposite. About the pitching up moment, the same tendency is present but with minimal variations, and it is not possible to notice any differences between the two shapes.

An increase of 10% in the diameter produces 17% to 19% of interference growing on the pitching up moment, whereas, on the drag and on the lift, the worsening is small. The larger impact on the pitching moment is explainable with the grater proximity of the sting to the flap.

The variation of the dimension was evaluated also at α=15°, observing that it has a greater impact on the coefficients than what happens at α=0°. The trend for the drag and the lift is almost the same as with α=0°. Interesting is the drastic reduction of pitching moment interference with the longer elliptic sting (144%), whereas this is not present with the circular shape. By increasing the diameter, the coefficient most negatively affected is the pitching moment.

Increasing the inclination of the vertical bar, the differences on the pressure distributions are really appreciable only with 15° of variation (this means that the bar is closer to the vertical axis). It is possible to see an increase of the pressure on the rear surface and on the upper one, especially in the rear part. Otherwise, on the bottom, it is not possible to notice strong differences see **Figure 10**. This, as already clarified, means a decrease of the drag and the lift while the pitching moment grows. The global result is an increase on the interferences, which should be taken into account.

http://dx.doi.org/10.5772/62241

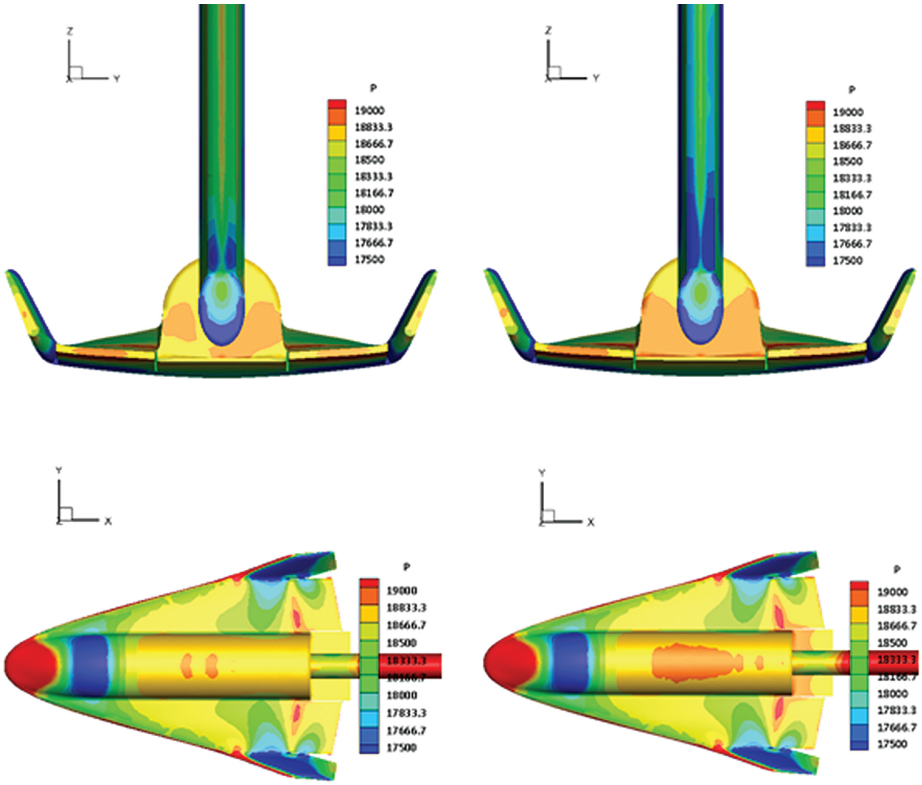

Figure 10. Different views of the SOAR with elliptic support. B=40.8° (left) and B=55.8° (right); scale 1:180, α=0°.

4.2.2. Scale 1:80

As expected, straight stings disturb less the flow than any supports with an inclined part. An increase of pressure on the model rear part due to the presence of the sting is present again but, because there are no large parts sticking out of the wake, the effects are small. The pressure that increases over the vehicle surface is much lower, but an increase on the rear surface of the SOAR is still present. This last phenomenon is more evident with the circular sting than with the elliptic one. Once again, the circular shape induces a larger blockage of the flow below the sting.

On the coefficients too, the straight sting induces the same kind of interferences, that is, the decrease of the drag and the lift and increase of the pitching moment. This time, the deviance with respect to the drag and to the lift from the SOAR alone is actually small see **Table 2**. For the pitching moment, greater interferences persist and, once again, the elliptic sting reacts better. This is due to the presence of the SOAR flaps under the sting that induces a higher pressure again.

Simulations	$\Delta C_{L\,av}$	$\Delta C_{D\,av}$	$\Delta C_{M\,av}$
SOAR with circular sting	0.00229	0.00254	−0.01434
SOAR with elliptic sting	0.00186	0.00217	−0.00857

Table 2. Average correction, respect of the angle of attack, on the coefficients when the support is present compared to the SOAR alone; scale 1:80

The 10% dimensional variations on the straight sting produce minimal differences on the pressure contours. Now a shorter sting causes a lower pressure on the vehicle rear surface with a behavior closer to the SOAR alone. The reasons for this are twofold. First, it should be remembered that turbulent flow at the model rear base predicts a shorter critical sting length (three to five times the base diameter) that is not possible to predict exactly. The sting length in scale 1:80 is 3.4·*D* and the critical sting length should be on the range of 10% variations. Second, with this model of sting, there are not any inclined parts out from the wake of the SOAR. In fact, the disturbances of the support, in scale 1:180, are bigger when the vertical part is closer to the vehicle, that is, with a shorter sting. On the contrary, with only a straight sting, the shorter it is, the lower are the perturbations on the wake, even if the amount of the interferences is always smaller. It is difficult to clarify this trend because in reality, at the end of the sting, there should be another structure usually with a larger diameter. The effect of this bigger diameter component can be similar to what induced an inclined bar, that is, to increase the flow blockage as closer to the vehicle. Now the effect on the coefficients is smaller and they usually remain approximately constant with some exceptions: on the lift, the elliptic longer sting reduces the interferences (29%), whereas the circular longer one increases (16%). On the pitching moment, the longer elliptic sting reduces the interferences by approximately 20%.

Increasing the diameter by 10% produces similar interferences to what happens in scale 1:180. Once again, the greatest deviances are observed for the pitching moment.

The variation of the dimensions at 15° angle of attack has a small impact on the drag and on the lift, whereas, on the pitching moment, there is a drastic reduction of interferences with both shapes. Increasing the diameter causes only a 20% growth of the deviation for the moment coefficient with respect to the SOAR alone.

4.3. Comparison with the previous support

It is useful to remember that this study and the support design rose from the necessity to build new supports after the first wind tunnel testing campaign in the VKI. All results of that research activity are found in Ref. [1].

The old support was attached to the vehicle from the top (dorsal strut) and it was discovered to induce high interferences. That support configuration induced an extra pressure in front of the sting and lower pressure on the side. Furthermore, lower pressures were presented on the back of the SOAR behind the body and on the top of the flaps. These pressure decreases induced large forces due to the big areas it was acting on with the double effect to increasing in the drag and generating a pitching down moment.

http://dx.doi.org/10.5772/62241

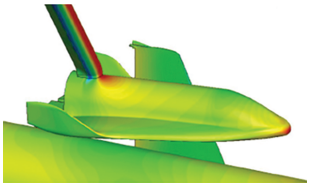

Figure 11. Sting effect on the old support. It is possible to see the red peak of pressure at the base of the sting; scale 1:180.

The previous separation wind tunnel tests were performed in scale 1:180, and the cases at 0 and 10° angle of attack are comparable with the results of this paper.

The use of the posterior supports dramatically reduces the interferences in terms of drag and lift with respect to the dorsal strut. On the contrary, the rear sting causes greater interferences to the pitching moment. Furthermore, the sting effect is opposite: whereas the drag was increased, now it is decreased, and the pitching moment now is higher, whereas before it was smaller. Also, the effect with the angle of attack is different: with the previous support, the amount of the correction was reduced increasing α, whereas the new models make the situation worse with high α. Only for the lift all choices cause decrease in the coefficient respect to the SOAR alone see **Table 3**.

	Old support			**New circular support**			**New elliptic support**		
α	ΔC_D	ΔC_L	ΔC_M	ΔC_D	ΔC_L	ΔC_M	ΔC_D	ΔC_L	ΔC_M
0	−0.0328	0.0662	0.0082	0.0045	0.0086	−0.0242	0.0039	0.0078	−0.0218
10	−0.0159	0.0891	0.0059	0.0058	0.0079	−0.0426	0.0046	0.0071	−0.0391

Table 3 Comparison of the performance between the support with circular and elliptic sting and the old one; scale 1:180, α=0°

4.4. Local pressure coefficient corrections

In this paragraph, the coefficient alterations are revised, but now looking at the pressure point by point. The following critical area of the vehicle are selected for this analysis: the rear surface, the body, and the flaps see **Figure 12**.

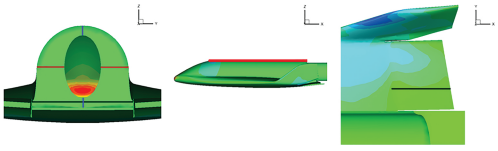

Figure 12. With different colors, the lines where the pressure are evaluated: left, the SOAR rear surface; middle, the body; right, the flap.

The main goal of the investigations is to find corrective coefficients to correct for the presence of the support with information coming from the pressure values. In fact, during the wind tunnel test, a small transducer will be positioned to measure the pressure at smart locations. With the coefficients found in this analysis, it will be possible to have a value of the local pressure corrected and then close to what happens without the support. Afterwards, it is desirable to apply these coefficients also at corrective laws for the aerodynamics coefficients. The sense of the last point is to have a quick way to obtain an indicative value of the coefficient correction for each case, which can be tested in the wind tunnel. The study is done for the nominal dimension geometry function of the angle of attack.

First, the local pressure values are presented, and after the correction, laws are explained.

4.4.1. Local pressure values

Regarding the rear surface and the upper body surface, what was already analyzed in the previous paragraph was confirmed. The circular sting induces higher pressure in the lower part of the rear surface, with a large peak and slightly lower value in the upper zone see (see **Figure 13**) Increasing the sting length, as expected, the pressure is closer to the values of the SOAR alone (see **Figure 9**). This is present with the same trend for both sting shapes in scale 1:180, not in scale 1:80 where the differences are small.

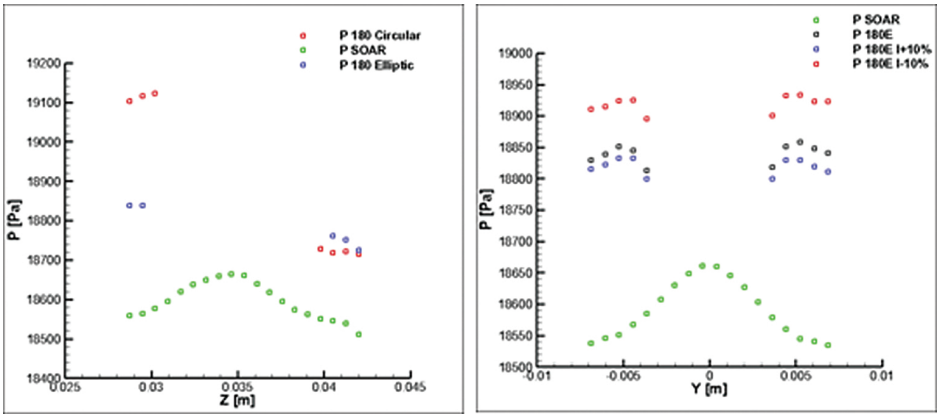

Figure 13. Rear surface pressure distribution plot: on the red line for the elliptic sting with different length (left) and on the blue line for SOAR alone and with different sting shapes (right); scale 1:180, α=0°.

On the body upper surface, the support creates an overpressure on the rear part of the vehicle, more evident in scale 1:180. The pressure is calculated also on the right flap in the longitudinal direction following the black line shown in **Figure 12**. As expected, the longer sting always has a lower correction than the shorter and the elliptic shape is closer to the SOAR alone (see **Figure 14**).

http://dx.doi.org/10.5772/62241

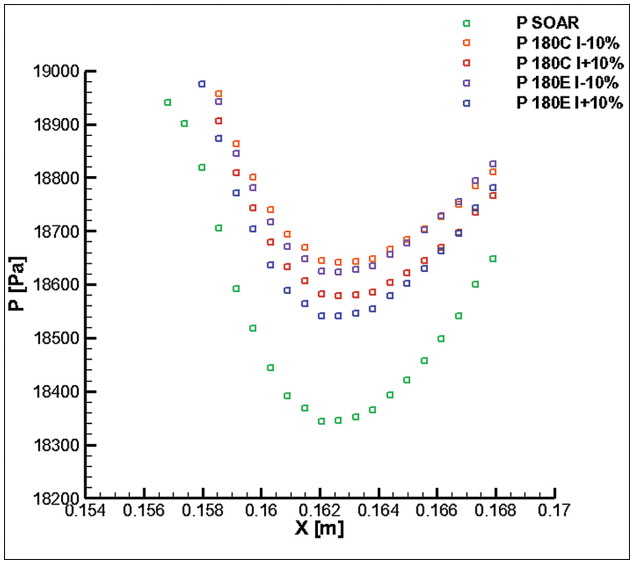

Figure 14. Pressure distribution on the flap for different shapes and geometries; scale 1:180, α=0°.

The impact of higher pressure on the flap is always towards increasing the pitching up moment. It is interesting to notice that the flap is more affected by the sting for α=0° than for α=15° and that the circular sting produces less interferences on it, increasing the angle of attack (see **Figure 15**). It is possible to find a similar trend also in scale 1:80, but the differences are minimal.

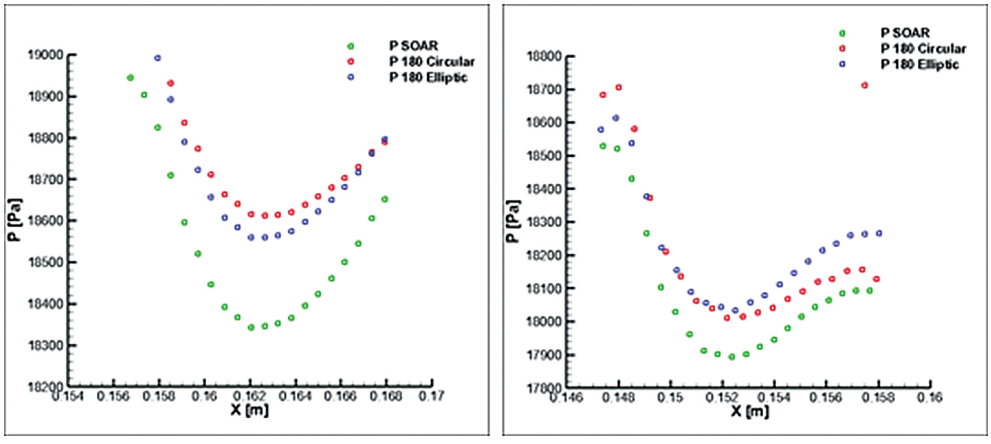

Figure 15. Pressure distribution with nominal dimensions on the flap, circular and elliptic sting; scale 1:180, α=0° (left) and α=15° (right).

4.4.2. Coefficients corrective laws

The coefficients coming from the simulations with support are corrected for the presence of the struts.

Scale	**1:180**		**1:80**	
Ki,j	Circular	Elliptic	Circular	Elliptic
Flap	0.989	0.990	0.996	0.997
Base	0.975	0.986	0.989	0.994

Table 4. Averaged local pressure ratio

The surface pressure alterations are considered responsible for the interferences on the coefficients, see Equation (1) and **Table 4**. The ratios ($K_{i,j}$) between the pressures, on the rear surface, of the SOAR alone divided by the same pressure when the support is present are taken into account to correct the drag. The same values on the flap surface are supposed to be determinant for the pitching moment and the lift. Afterwards from these pressure ratios a first correction coefficient is applied and then other elements are added to try to have the best fit of the simulation results.

$$K_{i,j} = \frac{P_{SoarAlone\,i,j}}{P_{SoarWS\,i,j}} \tag{1}$$

The corrected results always present a residual average error from the SOAR alone lower than 10^{-4}, and few cases have an error of 10^{-3}. The improvement from the results coming from the simulations is always at least one order of magnitude. It is useful to highlight that the nature of this correction is totally empiric.

For the drag, the pressure corrective coefficient is in the denominator because the higher pressure induced by the sting on the SOAR rear surface reduces the drag coefficient.

On the lift, the pressure coefficient multiplies the aerodynamics coefficient because the overpressure on the flap (and on the body) reduces the lift but making it less negative for α=0°.

For the pitching moment, the pressure coefficient is divided by a factor 10. This is for the huge impact that the flap overpressure has on the coefficient due to the distance from the CoG and the large surface. Then everything is multiplied to the moment coefficient because the sting effect is to increase it.

As example, just the drag and lift corrective law for the circular sting and the pitching moment corrective law for the elliptic one are reported, and all corrective laws are in Ref. [9]. All is referred to the scale 1:180.

http://dx.doi.org/10.5772/62241

$$C'_{D,C} = C_D \frac{1}{K_{b,C}} + 4{,}1174 \cdot 10^{-3} \tag{2}$$

$$C'_{L,C} = K_{f,C} C_L + 8.3573 \cdot 10^{-3} + 2.5311 \cdot 10^{-5} \alpha^{2,2} \tag{3}$$

$$C'_{M,E} = \frac{K_{f,E}}{10} C_M + 2.81817 \cdot 10^{-4}\, 8.511 \cdot 10^{-4} \alpha \tag{4}$$

5. Conclusions

All supports are structurally valid and induce an amount of interferences manageable with the suitable corrections. The conclusions about the interferences will now be analyzed more in detail.

The elliptic sting shape presents, in both scales, the best performance, especially on the pitching moment coefficient and at α=15°. For all supports with an angle of attack much higher than 10°, the usage of the elliptic sting is definitely suggested. In scale 1:180, there are evident advantages with its usage also on the drag and on the lift coefficients and also at the lower angle of attack. In scale 1:80 for all the coefficients, the interferences, in spite of the greater scale, are at least half of what happens with the 1:180 supports. For the lift and the drag, the differences between the two shapes are halved, with the same trend. The pitching moment worsening with α is reduced, especially for the elliptic sting.

Varying the dimensions, the trend is what was expected, in scale 1:180: the interferences go down increasing the length and decreasing the diameter. It is more complex in scale 1:80, as already discussed, and the range of alterations is not enough to clearly understand the behavior of the support. For the pitching moment having a sting 10% longer at 15° angle of attack dramatically reduces the interferences. The reason why this is not revealed for the circular sting in scale 1:180 is not clear yet.

Increasing the inclination of the vertical parts (only scale 1:180), the interferences increase. If the variation is 5°, the effect is minimal; at B=55.8°, the interferences rise more.

Comparing this to the old support (only scale 1:180), the first consideration is that the SOAR rear part, including their flaps, is a critical zone for the interferences. In fact, for their large flat surfaces, only small deviances on the pressure contour cause great alterations on the coefficients. This in particular affects the pitching moment for the distance from the CoG. Every kind of support will, more or less, produce alterations on the flow in this part and then a certain amount of interferences is inevitable. On the contrary, to have a support that does not interfere with the rear part is not possible. The dramatic reduction of drag and lift interferences, with a posterior sting, seems to be interesting even if it is necessary to take into account a worsening

of the pitching moment. With little optimization on the design, the use of an elliptic shape and the research of some expedient to reduce the moment interferences may be the best solution.

6. Recommendations for future activities

It is interesting to examine more in depth some aspects of this study such as the impact of shape and dimensional variation. To do this, it is useful to perform simulations at more angle of attacks and to apply greater length alterations. It is possible to do this remaining in the original constraints for the scale 1:80 where they are less severe.

Furthermore, for a more in-depth analysis, it is necessary to perform CFD test of supports with the completed sustaining mechanism. This is useful especially for the straight sting (scale 1:80) where testing only the last part of the support is not possible to clarify the interference variations with the length. Therefore, it will be possible also to understand better the influence of the Reynolds number on the length.

Another critical point is to research a solution to decrease the interferences on the pitching moment. To permit this in scale 1:80, there is the possibility to position the sting higher on the SOAR rear surface. This should reduce the flow blockage over the flaps. It is more difficult to realize the same in scale 1:180 (especially for the elliptic sting) for the higher ratio dsDalready existent.

Finally, it is also interesting to estimate the accuracy and the usefulness of the new correction methods purpose in Section 4.4.

Nomenclature

α angle of attack

B inclination angle of the support vertical part

CoG center of gravity

C' aerodynamics coefficient corrected for the effect of the support

D model base diameter

d sting diameter

$\mathbf{K_{i,j}}$ $K_{i,j} = \frac{P_{SoarAlone\ i,j}}{P_{SoarWS\ i,j}}$

LC critical sting length

l sting length

M Mach number

http://dx.doi.org/10.5772/62241

Re Reynolds number

VKI The Von Karman Institute for Fluid Dynamics

Author details

Alberto Ghiraldo[1*], Sebastien Paris[2] and Ernesto Benini[1]

*Address all correspondence to: albertoghiraldo@hotmail.it

1 University of Padua, Padua, Italy

2 The Von Karman Institute for Fluid Dynamics, Belgium

References

[1] Swiss Space System. SOAR design definition file design justification file. Internal document. 2013.

[2] S Paris, BànyaiT.. Contribution to the aerodynamic database of the SOAR and the Airbus A300 during the separation—wind tunnel tests and CFD. VKI Internal report. 2014;S3-VKI-RPT-001.

[3] FB Cyran. Base Pressure Measurement of the Standard Dynamics Model Aircraft at Mach Numbers 0.3 Through 1.3. Tennessee, USA: Arnold Air Force Station; 1981.

[4] A Pope. Wind Tunnel Calibration Techniques. AGARDograph; 1961.

[5] S Hoerner. Fluid Dynamic Drag; 1965.

[6] HM Schurmeier. An Investigation of the Interference Effect of a Sting Support System on the Pressure Distribution over a Body of Revolution. Pasadena, CA, USA: Pasadena Institute of Technology; 1949.

[7] JD Anderson Jr.. Fundamentals of Aerodynamics. 5th ed. New York: McGraw-Hill; 2011.

[8] DL Loving, AA Luoma. Sting Support Interference on Longitudinal Aerodynamic Characteristics of Cargo-Type Airplane Models at Mach 0.70 to 0.84. Langley Station, Hampton, VA, USA: Langley Research Center; 1967.

[9] A Ghiraldo Effetto del supporto in misurazioni in galleria del vento (in English; only abstract available). Padua thesis. 2015.